

The variability properties of X-ray steep and X-ray flat quasars

Fabrizio Fiore^{1,2,3}, Ari Laor⁴, Martin Elvis¹,
Fabrizio Nicastro^{1,2}, Emanuele Giallongo²

¹ Harvard-Smithsonian Center for Astrophysics, Cambridge MA 02138, USA

² Osservatorio Astronomico di Roma, Monteporzio (Rm) I00040 Italy

³ SAX Science Data Center, Roma, Italy

⁴ Physics Department, Technion, Haifa 32000, Israel

(version: 8pm 11 March 1998)

ABSTRACT

We have studied the variability of 6 low redshift, radio quiet ‘PG’ quasars on three timescales (days, weeks, and months) using the ROSAT HRI. The quasars were chosen to lie at the two extreme ends of the ROSAT PSPC spectral index distribution and hence of the $H\beta$ FWHM distribution. The observation strategy has been carefully designed to provide even sampling on these three basic timescales and to provide a uniform sampling among the quasars

We have found clear evidence that the X-ray steep, narrow $H\beta$, quasars systematically show larger amplitude variations than the X-ray flat broad $H\beta$ quasars on timescales from 2 days to 20 days. On longer timescales we do not find significant differences between steep and flat quasars, although the statistics are poorer. We suggest that the above correlation between variability properties and spectral steepness can be explained in a scenario in which the X-ray steep, narrow line objects are in a higher L/L_{Edd} state with respect to the X-ray flat, broad line objects.

We evaluated the power spectrum of PG1440+356 (the brightest quasar in our sample) between 2×10^{-7} and $\sim 10^{-3}$ Hz, where it goes into the noise. The power spectrum is roughly consistent with a $1/f$ law between 10^{-3} and 2×10^{-6} Hz. Below this frequency it flattens significantly.

Subject headings: quasars — variability, X-rays, emission lines

1. Introduction

While X-ray variability in Seyfert galaxies has been the subject of intensive study (see review by Mushotzky, Done & Pounds 1993, and Green et al 1993, Nandra et al. 1997), the variability of quasars, being fainter, have received far less attention (the Zamorani et al. 1984 study remains the most extensive to date). Higher luminosity AGN had been expected to be physically larger and so have slower, and most likely lower amplitude, variations. A typical quasar is 100–1000 times more luminous than the highly variable Seyferts, such as NGC 4051, and so would vary at a significantly lower rate, i.e. a minimum of several days. It was probably this expectation that deterred extensive observing campaigns. This is unfortunate since we show here that X-ray variability is common, rapid and of quite large amplitude (\gtrsim factor of 2). The variability most likely originates in the innermost regions of quasar, and so can help unravel the basic parameters of the quasar central engine (mass, geometry, radiation mechanisms, radiative transfer) none of which are yet well constrained.

These speculations are supported by compact galactic sources, for which the investigation of the “variability properties vs. spectral shape” and the “variability properties vs. luminosity” planes have brought a great improvement in our understanding (see e.g. van der Klis 1995). The same is likely to happen for quasars. Compact galactic sources are usually bright and variable on timescales as short as 1 ms, which means that their variability timescales can be probed by just a few observations of individual objects. For example, the Galactic black hole candidate (BHC) Cyg X-1 recently underwent two dramatic changes in its variability and spectral properties (see e.g. Cui et al. 1997), and it was possible to follow the whole cycle from the usual low and hard state, to a medium-high, softer state, and back to the low and hard state in the course of a few months. This is unlikely to happen in a luminous AGN, even if there were similarities between AGN and black hole candidates, because the variability timescales (and the sizes and luminosities) are probably much longer (greater and higher) in AGN. Instead, if the analogy between quasars and BHC holds, we will observe a population of quasars some in a ‘high and soft’ state, and some in a ‘low and hard’ state.

Hence the analogous observational way forward in quasars is to investigate the variability properties of samples of quasars, selected according to their spectral properties and luminosity.

The evidence for rapid, large amplitude, X-ray variability in a few AGN with unusually steep X-ray spectra and unusually narrow Balmer lines (mostly Narrow Line Seyfert 1 galaxies, NLSy1, given the strong correlation between these two quantities found by Laor et al., 1994, 1997, Boller, Brandt & Fink 1996) has recently grown:

1. NGC4051 shows large variations (50 %) on timescales of ≈ 100 seconds and has very narrow optical and UV emission lines and steep 0.1-2 keV X-ray spectrum. It is also highly variable in the EUV (a factor of factor of 20 in 8 hours, Fruscione et al 1998).
2. IRAS13224-3809 has a particularly steep 0.1-2 keV spectrum ($\alpha_X > 3$) narrow $H\beta$ line, very strong FeII emission and shows X-ray variations of a factor 50 or more on timescales of a few days (Otani 1995, Brandt et al. 1995, Boller et al 1997) and a factor of 2 in less than 800 seconds (Boller et al. 1996);
3. RE J 1237+264 showed one very large (factor of 50) variability event (Brandt, Pounds & Fink, 1995)
4. PHL1092 varied by a factor of 4 in 2 days (Forster & Halpern 1996, Lawrence et al. 1997). PHL1092 is a high luminosity (5×10^{46} erg s $^{-1}$) very steep 0.1-2 keV spectrum and narrow emission line quasar.
5. The relatively high luminosity quasar NAB0205+024 ($L_{0.5-10keV} = 8 \times 10^{44}$ erg s $^{-1}$) shows variations of a factor of 2 in less than 20 ks in an ASCA observation (Fiore et al. 1998a).
6. Mark 478 (PG1440+356) shows factor of 7 variations in 1 day during a long EUVE monitoring (Marshall et al 1996)
7. The extremely soft NLSy1 WPVS007 ($\alpha_{0.1-2keV} = 7.3$) showed a huge variation (factor of 400) variation between the RASS observation and a follow-up PSPC pointed observation taken 2 years later (Groupe et al. 1995).

At this point we believe that a systematic study of a sample of normal quasars spanning the observed range of properties is needed. A systematic study of the variability properties of AGNs is not an easy task, since it requires:

1. the selection of well defined and representative (i.e. unbiased) sample;
2. the availability of numerous repeated observations;
3. a carefully designed observational strategy. In particular, it is very important that the sampling time is regular and that it is similar for all objects in the sample, so that the results on each object can be easily compared with each other. Otherwise the differences in the observed variability may be induced just by differences in sampling patterns.

Because of these stringent requirements systematic studies are still lacking (for example the Zamorani et al. 1984 study on quasars, and the Green et al. 1993 study on Seyfert galaxies do not fulfill any of the three criteria above). To explore in a systematic manner the possible relation between line width, soft X-ray spectrum and X-ray variability properties, we initiated a pilot program using the ROSAT HRI. In the following we present the results from a campaign of observations of six PG quasars which addresses the above points.

2. The sample

Six quasars were chosen from a complete sample of 23 optically selected (PG) quasars ($M_B < -23$), all studied with the ROSAT PSPC (Laor et al. 1994, 1997). To maximize the rest frame soft X-ray detectability in the whole 0.1-2 keV PSPC band the Laor et al. sample of PG quasars ($M_B < -23$) is limited to quasars with: low redshift ($z < 0.4$) and low Galactic N_H ($< 1.9 \times 10^{20} \text{cm}^{-2}$). This sample of AGN has the advantage that it is extracted from a complete sample of optically selected quasars, and should therefore be representative of such quasars. In particular, the Laor et al. sample selection criteria are independent of the X-ray properties, and thus the sample is free from X-ray selection biases.

The six quasars were chosen to lie at the two extreme ends of the PSPC spectral index distribution ($f_\nu \propto \nu^{-\alpha_X}$, $1.2 \lesssim \alpha_X \lesssim 2.1$) and hence of the $H\beta$ FWHM distribution. Figure 1 show the $H\beta$ FWHM as a function of α_X for the radio quiet quasars in the Laor et al sample. (We excluded the X-ray weak quasar PG1001+054 which is too faint for followup variability studies with the HRI). X-ray steep and flat quasars discussed in this paper are identified by filled squares and open circles respectively. The quasar with $\alpha_X < 1$ and large errors is PG1114+445, which has an ionized absorber along the line of sight (Laor et al. 1997, George et al. 1997).

Objects with extreme properties should help highlight the basic correlations which may provide important hints for the underlying physical processes. Table 1 gives the redshift, the PSPC energy index, the 2 keV and 3000 Å luminosities (for $H_0 = 50 \text{ km s}^{-1} \text{ Mpc}^{-1}$, $q_0 = 0.5$) and the $H\beta$ FWHM for the six quasars. All the chosen quasars are radio-quiet.

3. The observational strategy

The observational strategy was designed to: a) provide even sampling on three basic timescales (days, weeks, and months), b) provide a uniform sampling among the quasars, and c) keep the total integration time reasonably small. These constraints result in a quasi-

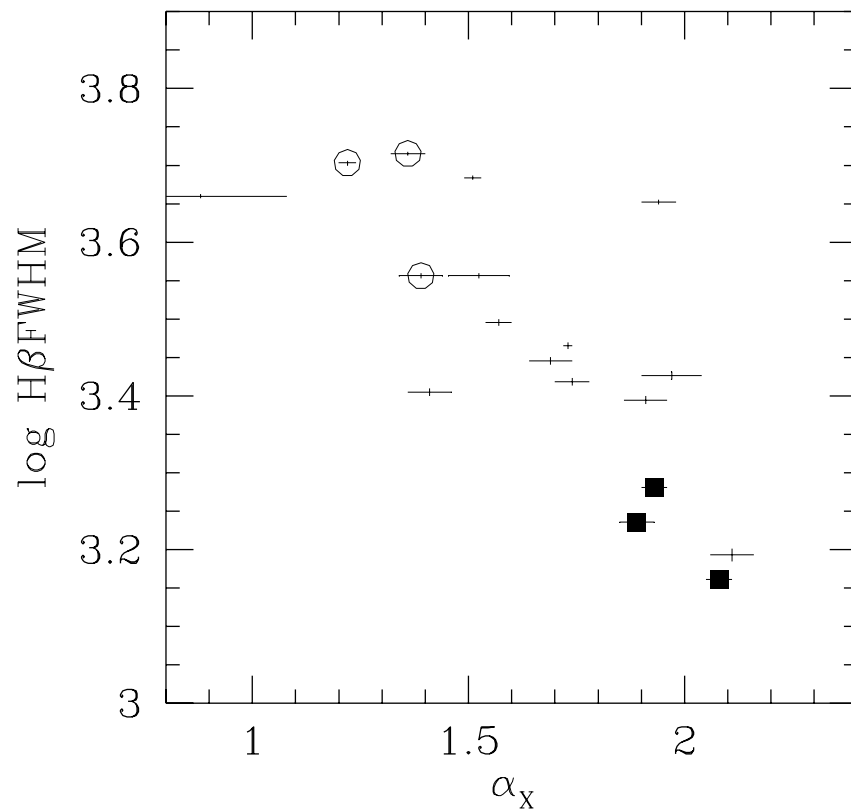


Fig. 1.— H β FWHM as a function of α_X for the quasars in the Laor et al sample. Filled squares and open circles identify the three X-ray steep and the three X-ray flat quasars discussed in this paper.

Table 1: Continuum and Line Parameters

name	z	α_X	$\nu L_\nu(2keV)$ erg s ⁻¹	$\nu L_\nu(3000\text{\AA})$ erg s ⁻¹	H β FWHM km s ⁻¹
Steep X-ray quasars					
PG1115+407	0.154	1.9	43.61	44.96	1720
PG1402+261	0.164	1.9	44.08	45.45	1910
PG1440+356	0.077	2.1	43.64	44.91	1450
Flat X-ray quasars					
PG1048+342	0.167	1.4	43.85	45.14	3600
PG1202+281	0.165	1.2	44.25	45.00	5050
PG1216+069	0.334	1.4	44.78	45.94	5190

logarithmic observation plan: one ~ 2000 s exposure a day for one week; one ~ 2000 s exposure each week for one month; two ~ 2000 s exposures a month apart, 6 months after the main campaign, i.e. 6-7 points with an *even* spacing of 1 day; 4-5 points with an *even* spacing of 1 week 2 points with a spacing of 1 month and 2 sets of 2 points with a spacing of 6 months. The S/N obtained allows the 3σ detection of $\sim 30\%$ variability in the faintest source of the sample.

4. Results

Tables 2 and 3, respectively, give the observation date, the net HRI exposure and the background subtracted HRI count rate for the X-ray steep and flat quasars. Counts were extracted from a region of 60 arcsec radius. Since $\sim 90\%$ of the counts from a point source fall within the same extraction region (David et al. 1997) no correction has been made for lost flux. Background was extracted from two 60 arcsec radius regions straddling the source region. The background is small in all cases (< 10 counts ks⁻¹ in a 60 arcsec radius regions).

We have also looked at longer variability timescales (of the order of 2000 days) by comparing the HRI fluxes with the PSPC fluxes obtained during the Rosat All Sky Survey (RASS) and the pointed ROSAT PSPC observations reported in Laor et. (1997). We converted the PSPC count rates to effective HRI count rates by assuming the spectral shape observed in the ROSAT pointed observations (Laor et al. 1997). RASS and pointed PSPC observations ‘converted’ count rates are given in Table 4.

4.1. Logarithmic normalized light curves

Figure 2 shows the logarithm of the light curves of the six quasars, each normalized to the mean flux, spanning about one month each, while figure 3 shows the observations performed six months later compared with the average flux and the dispersion observed on timescales shorter than one month. Figure 4 shows the normalized RASS and PSPC pointed observation points, the dispersion as in Figure 2 and the normalized HRI observation performed 6 months later.

The steep α_X quasars show large variations (up to a factor of 2) on all the timescales investigated. Conversely, the flat α_X quasars show little variability on short timescales. Factor of 2 variations with respect to the average flux seem to be allowed for both X-ray steep and X-ray flat quasars on 200-2000 days timescales, although the statistics on these timescales are poorer.

4.2. Structure function

To compare the variability of the quasar groups more quantitatively we computed the logarithm of the ratio between each pair of flux measurements (at two times t_i and t_j in the quasar rest frame). We then computed the median and the mean in 9 time bins for both flat and steep X-ray quasar samples:

$$(1) \quad < \Delta m > = \text{median or mean}(|2.5 * \log(f(t_j)/f(t(i)))|).$$

The function using the mean is similar to the so called ‘average structure function’ (see e.g. Di Clemente et al. 1996).

We have verified that no single quasar dominates the median and mean in eq. (1).

$< \Delta m >$ for the median is shown in figure 5. Error bars represent here the semi interquartile range. $< \Delta m >$ for the mean is shown in figure 6. Error bars represent here the error on the mean and are therefore less conservative.

It is clear that the $< \Delta m >$ (both mean and median) for X-ray steep quasars is significantly higher than that of X-ray flat quasars on timescales from 2 days to 20 days. On the longest timescale (200 days) the two $< \Delta m >$ are consistent with each other, with large errorbars. The point at about 2000 days in figures 5 and 6 compares the HRI monitoring results with the RASS results. The point at about 1000 days compares the HRI monitoring

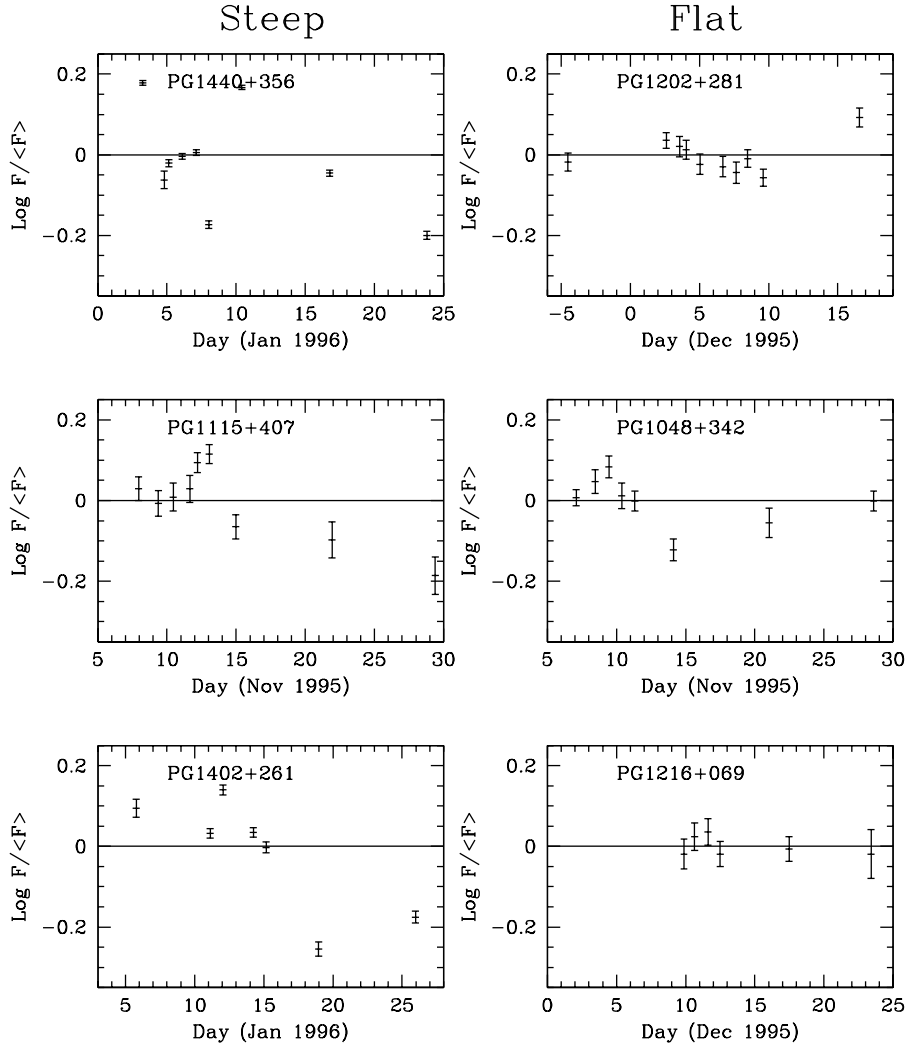


Fig. 2.— The ROSAT HRI light curves (plotted as logarithm of the ratio of the flux to the average flux) of the six quasars on a 2-20 day timescale.

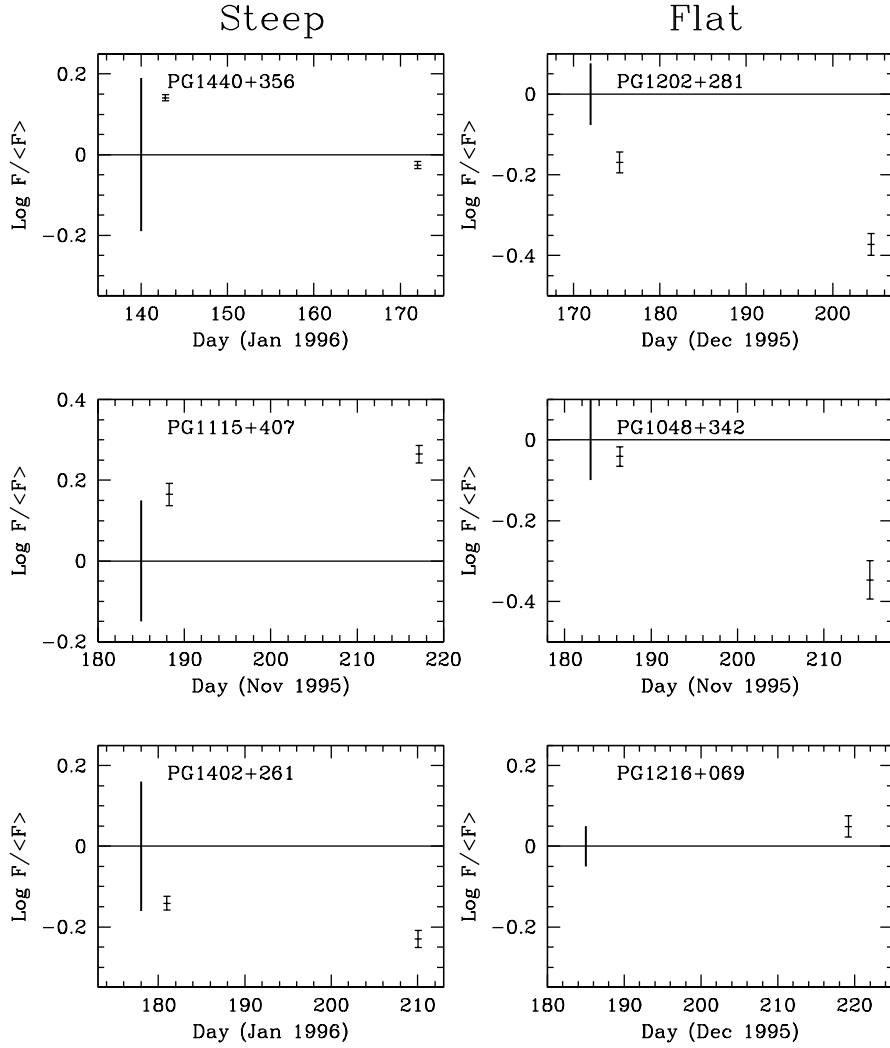


Fig. 3.— The HRI observations of the six quasars performed six months later compared with the average flux and the dispersion observed on timescales shorter than one month (20-200 days timescale).

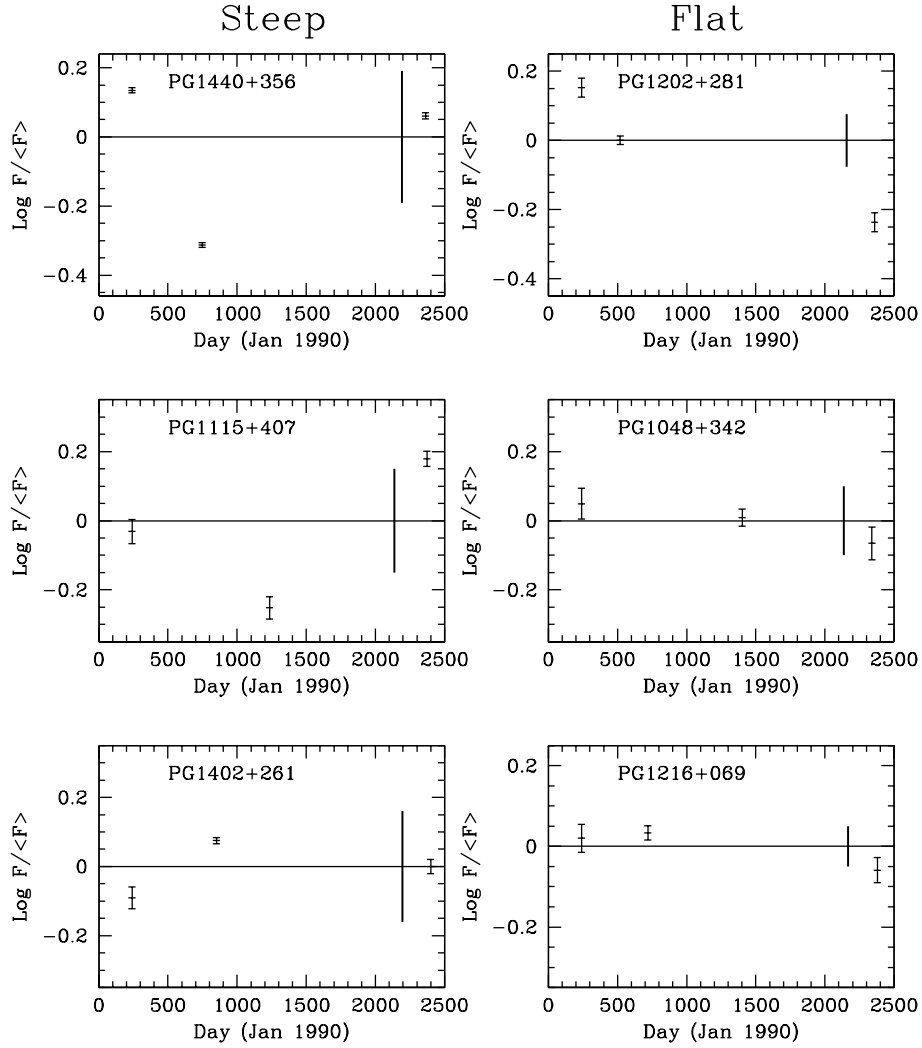


Fig. 4.— The HRI observations of the six quasars compared with the RASS and with the PSPC pointed observations (200-2000 days timescale).

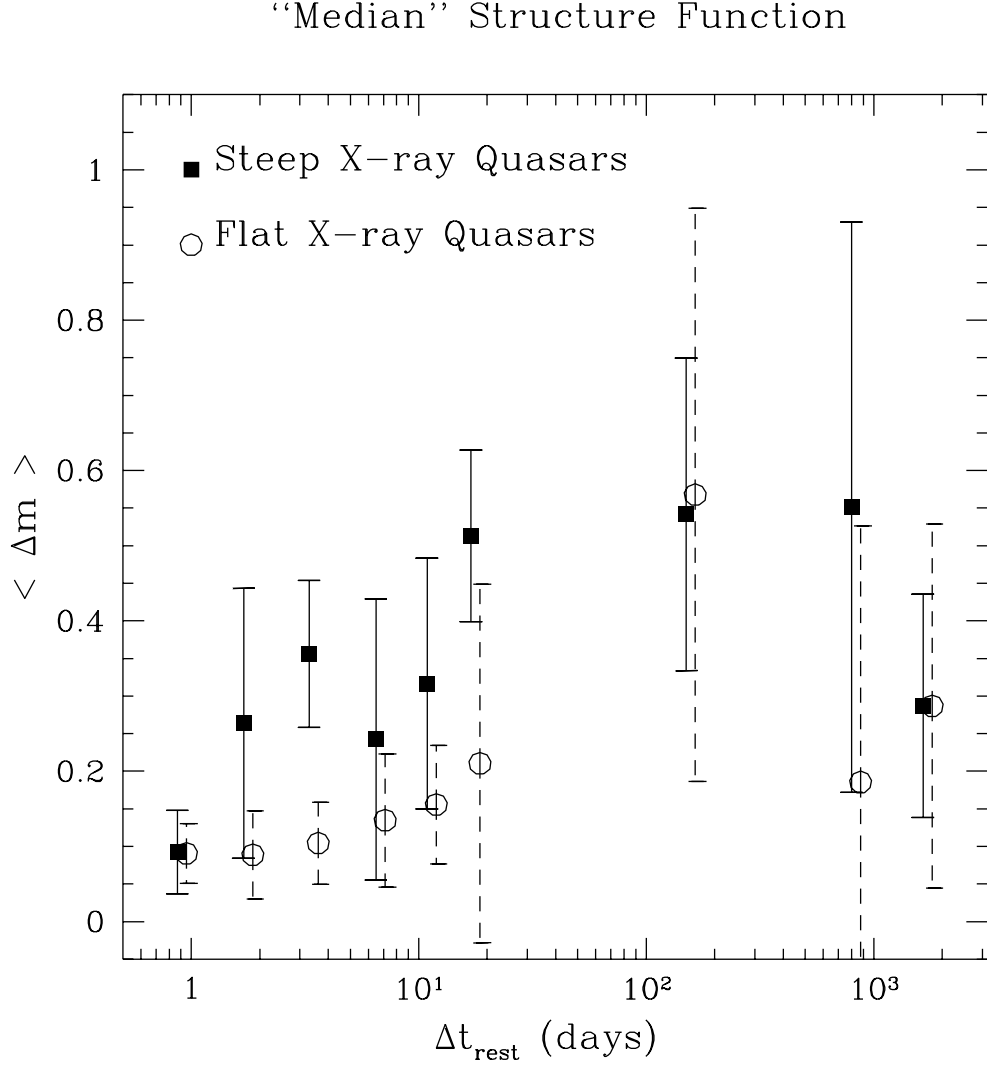


Fig. 5.— “Median” Structure Function ($\langle \Delta m \rangle$, see eq. 1) for the X-ray steep (filled squares) and flat (open circles). X-ray flat quasars points have been slightly shifted from real Δt for a sake of clarity.

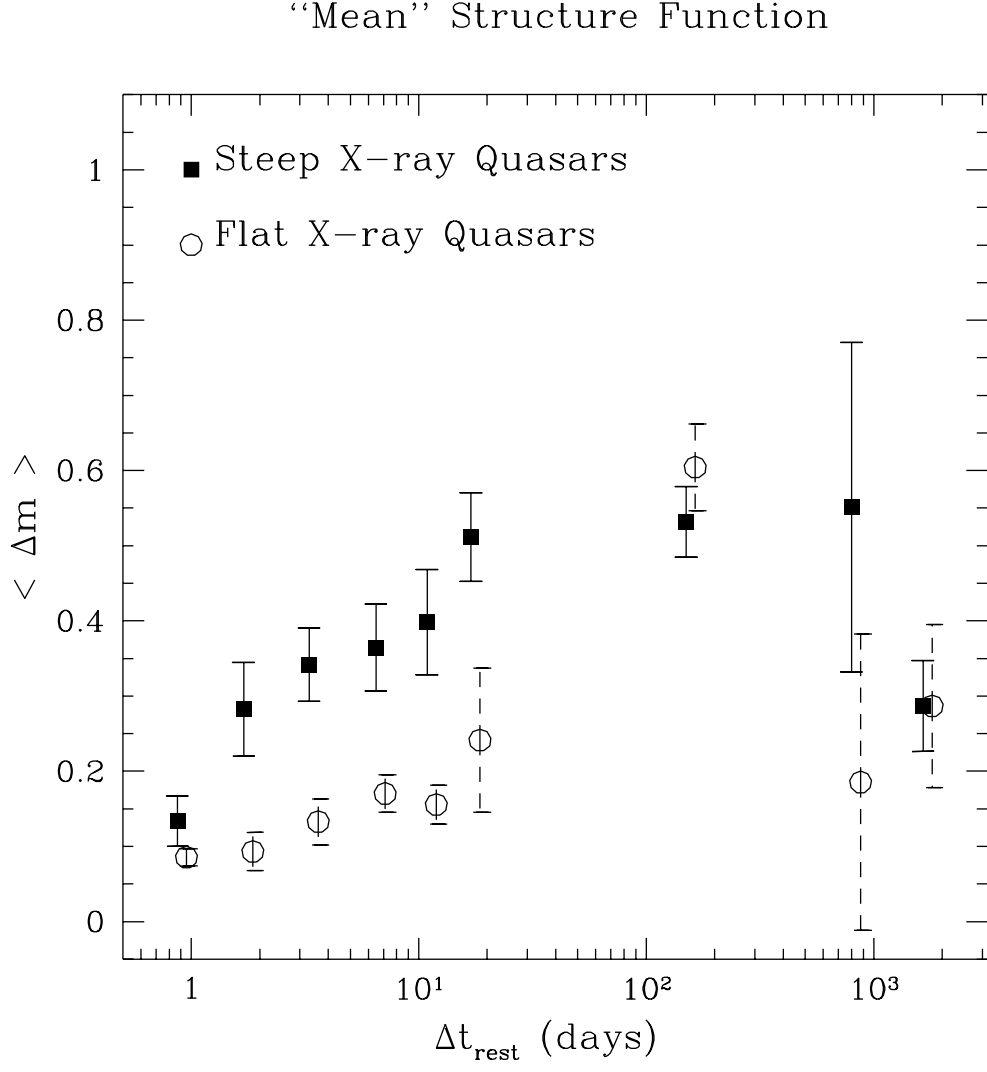


Fig. 6.— Mean Structure Function ($\langle \Delta m \rangle$, see eq. 1) for the X-ray steep (filled squares) and flat (open circles). X-ray flat quasars points have been slightly shifted from real Δt for a sake of clarity.

and the RASS results with the ROSAT PSPC pointed observations. The error bars here are larger because of the different sampling times used.

4.3. Power spectrum of PG1440+356

For the brightest quasar in our sample (PG1440+356) it is possible to investigate timescales shorter than the duration of each single HRI exposure. Analysis of the HRI light curves of each single OBI reveals significant variability down to a time scale of a few hundred seconds. To quantify the amplitude of this variability we have computed a power spectrum for each of the single HRI exposures and, to improve the statistics, we have added together the 12 power spectra. The resulting coadded power spectrum is shown in figure 7, along with the lower frequency power spectrum calculated at four reasonably well sampled frequencies using the full HRI monitoring. The error bars represent the dispersion of the power in each bin.

The power spectrum above 10^{-3} Hz is flat, and thus consistent with white noise. Excess power is detected at $\sim 5 \times 10^{-4}$ Hz, which is a factor ~ 100 smaller than that detected at $\sim 5 \times 10^{-6}$ Hz, a mean $1/f$ distribution. Unfortunately we do not have information on the power in the decade between 10^{-5} and 10^{-4} Hz and therefore we cannot tell whether the power spectrum decreases smoothly as $1/f$ above $\sim 5 \times 10^{-6}$ Hz or rather if it breaks at an intermediate frequency. Continuous monitoring up to several days is needed to answer to this question.

The uncertainty on the power below 10^{-6} Hz is large and then we cannot assess whether the power spectrum stays constant below this frequency or rather decreases, as suggested by the low frequency point in figure 7. We can however exclude that the power spectrum continues to increase as $1/f$ below 10^{-6} Hz, although the precise break frequency is ill defined. Systematic monitoring on weeks to months timescales can strongly constrain this frequency. In the framework of accretion disks models, this timescale may be related with the thermal or viscous instabilities, and its measure could help to estimate important model parameters like the mass of the central black hole and the viscosity parameter α (e.g. Siemiginowska & Czerny 1989)

5. Comparison with other work

Nandra et al. (1997) used the source root mean square variation σ_{rms}^2 from ASCA SIS data for a sample of (X-ray bright) AGN to suggest an inverse relation between variability

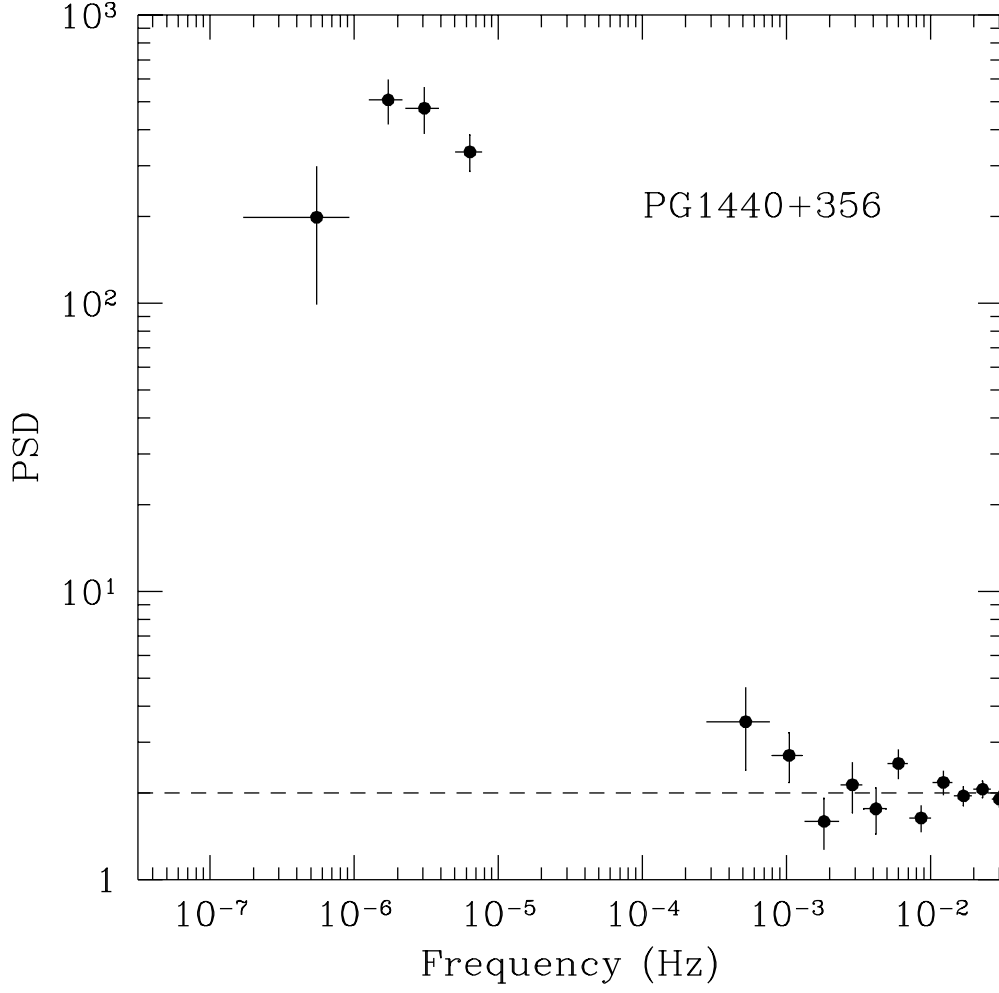


Fig. 7.— The power spectrum of PG1440+356 from 0.03 to 2×10^{-7} Hz. The power spectrum is normalized such that the level of the noise is 2 (dashed line).

and X-ray luminosity. Our sample of high luminosity, optically selected objects allows us to test this suggestion. We have calculated the noise subtracted σ_{rms}^2 according to the method of Nandra et al (1997). These are reported in Table 5 for two different time scales: days and months-to-years. (We do not show errors on σ_{rms}^2 because the analytic formula provided by Nandra et al. 1997 is not valid in the limit of small number of points.) The light curve of PG1216+069 in 2 is consistent with a constant value and therefore σ_{rms}^2 is formally zero in this case. We take the value of σ_{rms}^2 calculated for the other flat X-ray quasars (≈ 0.01) as an upper limit of σ_{rms}^2 in PG1216+069.

Figure 8 shows σ_{rms}^2 as a function of the X-ray luminosity and of the soft (0.1-2 keV) X-ray spectral index for the six quasars in our study and for the sources in Nandra et al (1997) with no strong low energy absorption (to provide a low energy X-ray spectral index). For this figure we used the σ_{rms}^2 SIS 0.5-2 keV in Nandra et al (1997). This band overlaps quite well with the HRI band (the HRI has some response in the ‘carbon’ band, below 0.3 keV, but this is much smaller than in the 0.5-2 keV band). The PSPC spectral indices for the Nandra et al. objects are taken from Walter & Fink (1993) and Laor et al (1997) or are calculated from WGACAT hardness ratios when not available in these papers. The variability of the Nandra et al. objects was measured on a time scale of $\sim 1 - 4 \times 10^4$ s, i.e. about an order of magnitude shorter than the timescales probed for the PG quasars (for the six PG quasars σ_{rms}^2 in figure8 refers to the 2-20 days time scale).

The addition of the six quasars makes a substantial difference. For the Nandra et al. sample alone the σ_{rms}^2 vs L_{1keV} linear correlation coefficient is $r=-0.82$ (probability of 99.9 %), while with the quasars it is reduced to $r=-0.54$. This is still significant (probability of 95 %), although it depends entirely on one point (the low luminosity Seyfert 1 galaxy NGC4051). The values of σ_{rms}^2 and α_X were uncorrelated for the Nandra et al. sample alone ($r=+0.37$, probability of 15%); adding the quasars results in $r=+0.55$, a 95 % probability correlation.

At a given luminosity the three x-ray ‘steep’ quasars from our sample all have σ_{rms}^2 higher than both the ‘flat’ X-ray quasars in our sample and all the other objects in the Nandra et al. (1997) sample by a factor of 10 to 100. The σ_{rms}^2 for the Nandra et al. (1997) sample refers to a factor of ten smaller timescale, and this might explain why they show lower amplitude variability for the same X-ray luminosity. However, if the power spectrum of the steep X-ray spectrum quasars falls like $\approx 1/f$ on the 0.1 to 1 day timescales (as suggested for PG1440+356, see §4.3), then only part of the difference in σ_{rms}^2 could be explained. If the power spectrum stays more or less constant on these timescales then this difference is highly significant. A comparison of variability amplitude in this frequency range between broad and narrow line Seyfert galaxies using ASCA and BeppoSAX light curves of similar

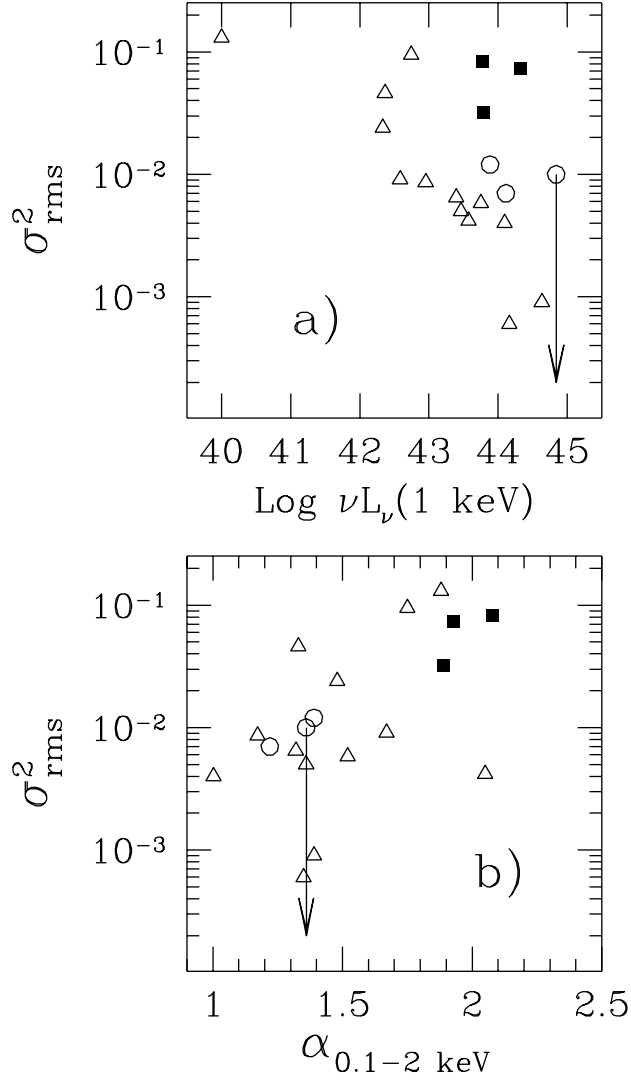


Fig. 8.— The ‘excess’ variance as a function of the 1 keV luminosity (in $\text{erg s}^{-1} \text{Hz}^{-1}$) and of the 0.1-2 PSPC spectral index. Open triangles show quasars and Seyfert galaxies from Nandra et al. 1997, filled squares identify steep X-ray spectrum quasars, open circles identify flat X-ray spectrum quasars.

sampling and length is in progress and will be part of a forthcoming paper (Fiore et al. 1998, in preparation).

Finally we note that the 1 keV X-ray luminosity and the spectral index are slightly anti-correlated ($r=-0.20$) in the sense that steeper objects tend to have lower 1 keV luminosities. The correlation is not significant here, but Laor et al. (1997) find a more significant correlation between α_X and the 2 keV luminosity in their complete, optically selected sample of PG quasars ($r_s = 0.482$, probability of 98 %). Thus, low luminosity AGNs tend to be more variable because of the luminosity-variability correlation, but on the other hand they also tend to have flatter spectra, which diminishes their variability due to the spectral index-variability correlation. To remove the effect of the $\alpha_X - L_x$ correlation from the $\sigma_{rms}^2 - L_x$ and $\sigma_{rms}^2 - \alpha_X$ correlations we performed a partial correlation analysis (e.g., Kendall & Stuart 1979). The correlation coefficients turns out to be very similar to the previous ones (-0.53 and 0.54), giving a probability for a correlation again of 95 %. This is still a marginal result, which could be highly strengthened or weakened by adding just a few more points at low and high luminosities and at flat and steep α_X .

A correlation between variability and spectral shape, similar to that discussed in this paper, has been reported also by Green et al. (1993) and König, Staubert and Timmer (1997) in two different analyses of EXOSAT lightcurves of AGN.

Di Clemente et al. (1996) studied the variability of 30 PG quasars in the red band and compared it with that of a sample of 21 PG quasars observed by IUE. Their full sample contains 39 quasars, the majority of which (24) at $z < 0.4$, as the quasars discussed in this paper. Three of the six quasars discussed in this paper are also part of the Di Clemente et al sample (the three X-ray flat quasars). Di Clemente et al. found that the variability amplitude increases with the rest frame frequency on both 0.3 and 2 years timescales. Extrapolating their correlation in the X-ray band one would predict a $\langle m \rangle$ of 0.75 and 0.83 for the 2 timescales. This is somewhat surprisingly close to the measured $\langle m \rangle$ on these timescales, given that variability in the red band, UV and X-ray may well have a completely different origin.

6. Discussion

In our sample of six PG quasars we found clear evidence that X-ray steep quasars show larger amplitude variations than X-ray flat quasars on timescales from 2 days to 20 days. On longer timescales we do not find significant differences between steep and flat quasars, although the statistics are poorer. While the sample in this pilot study is small

(and expanded monitoring of a larger sample of quasars is surely needed), the distinction is so clean cut that we feel justified in speculating on its origin.

Large narrow band flux variability in sources with a steep spectrum could be induced by small changes in the spectral index without large variations of the spectrum normalization. If this is the case each source should show large spectral variability, with α_X anti-correlated (correlated) with the observed flux if the pivot is at energies lower (higher) than the observed band. Spectral variability of this kind has not been observed in the PSPC observations of these and other quasars (Laor et al. 1997, Fiore et al. 1994) and in NLSy1 (Boller et al 1997, Fiore et al. 1998a, Brandt et al. 1995). Although our HRI observations cannot directly rule out this possibility, we therefore conclude that the observed temporal variability pattern is not likely the result of complex spectral variability.

Laor et al (1997) suggest that a possible explanation for the remarkably strong α_X – H_β FWHM correlation is a dependence of α_X on L/L_{Edd} . The line width is inversely proportional to $\sqrt{L/L_{\text{Edd}}}$ if the broad line region is virialized and if its size is determined by the central source luminosity (see Laor et al. 1997, §4.7). So narrow-line, steep (0.1-2 keV) spectrum AGNs emit close to the Eddington luminosity and have a relatively low mass black hole. A similar dependence of spectral shape on L/L_{Edd} is seen in Galactic black hole candidates (BHC) as they change from the ‘soft-high’ state to the ‘hard-low’ state.

A physical interpretation for this effect, as described by Pounds et al. (1995), is that the hard X-ray power-law is produced by Comptonization in a hot corona and that as the object becomes more luminous in the optical-UV, Compton cooling of the corona increases, the corona becomes colder, thus producing a steeper X-ray power-law. In BHC in ‘soft-high’ states this power law component emerges above ~ 10 keV, while the spectrum below this energy is dominated by softer emission often associated with optically thick emission from an accretion disk. In this model quasar disc emission is at a too low an energy to observe, since the disc temperature scales with the mass of the compact object as $M_{\text{BH}}^{-1/4}$, leaving the Comptonized power law to dominate the 2-10 keV spectrum. The 0.2-2 keV quasar emission could be due to Comptonization (see e.g. Czerny & Elvis 1987 and Fiore et al. 1995) by a second cooler gas component. The 0.2-2 keV and 2-10 keV spectral indices might well be correlated with each other, if the emitting regions are connected or if the emission mechanisms know about each other. We have undertaken a campaign of observations of the quasars in the Laor et al. (1997) sample with ASCA and BeppoSAX to clarify this point. Preliminary results (Fiore et al. 1998b) shows that this is indeed the case: steep α_X (PSPC) quasars tends to have a steeper hard (2-10 keV) X-ray power-law (although the spread of the 2-10 keV indices seems smaller than that of the PSPC indices (as also found by Brandt et al. 1997)).

In a sample of quasars with similar luminosities, those emitting closer to the Eddington luminosity will also be those with the smaller black hole and hence smaller X-ray emission region. Thus light travel time effects would smear intrinsic X-ray variability up to shorter time scales in high L/L_{Edd} objects, compared with low L/L_{Edd} objects. Based on this interpretation, and on figures 5 and 6 it appears that the emission region of the steep soft X-ray quasars is a factor of ≈ 10 smaller than that of flat soft X-ray quasars (about $\approx 10^{16}$ cm and 10^{17} cm respectively). Alternatively, the higher variability of steep spectrum objects may be a true intrinsic property, which could be induced by some increased instability in high L/L_{Edd} objects. The range of luminosity in our sample is too small to tell if the variability amplitude appears to be better correlated with black hole mass, as expected for light travel time smearing, or with L/L_{Edd} , which would indicate an intrinsic mechanism.

It is interesting to note that a completely different analysis, based on the interpretation of the optical to X-ray spectral energy distribution in terms of emission from accretion disks also suggest a small black hole mass and an high accretion rate in two NLSy1 (Siemiginowska et al. 1998).

It is also interesting to note that Cyg X-1 in the “high and soft” state (Cui et al. 1997) shows a total root mean square variability higher than that measured during periods of transitions and in the “low and hard” state. This is due to strong $1/f$ noise, extending down to at least a few 10^{-3} Hz, when the source is the “high and soft” state (Cui et al. 1997). When the source is in the “low and hard” state this $1/f$ noise is not present (see e.g. the review of van der Klis 1995).

Ebisawa (1991) found in a systematic study of Ginga observations of 6 BHC that the time scales of variability for the soft and hard components are often different. The soft component is usually roughly stable on time scales of 1 day or less, while the hard component exhibits large variations down to msec time scales. If the time scales of BHC and quasars scale with the mass of the compact object the above two time scales translate to 10^4 years and 0.1 day respectively for our quasar sample. For a sample of quasars with similar redshifts and luminosities this predicts a rather small scatter in the soft component and a bigger scatter in the hard component. ROSAT results go in this direction. Laor et al. (1994, 1997) find that (for their sample of 23 low- z PG quasars) the scatter in the normalized 2 keV luminosity is significantly larger than that in the 0.3 keV luminosity.

We conclude that the analogy between AGN and Galactic BHC seems to hold qualitatively for their X-ray variability properties.

An alternative and intriguing possibility to explain the correlation between X-ray variability amplitude and spectral shape is that a component generated closer to the black hole

dominates the emission of steep α_X quasars, as in the spherically converging optically thick flow proposed by Chakrabarti and Titarchuk (1995) to characterize BHC in the high and soft state. If this is the case then we would again expect that the spectrum of the steep α_X quasars remain steep above 2 keV (and up to $m_e c^2$ according to Chakrabarti and Titarchuk). Observations with the ASCA and BeppoSAX satellites instruments, which are sensitive up to 10 keV, (Brandt et al 1997, Fiore et al 1998b, Comastri et al 1998) suggest that this is indeed the case.

Schwartz and Tucker (1988) suggested that AGN emission can be produced by an ensemble of acceleration sites (i.e. shock waves) with different electron spectral indices and therefore emitting power laws with different photon indices. In this picture the spectrum is a quadratic function in $\log E$ and the mean index at a given energy arises from the greatest number of individual acceleration sites. Variability would be greatest for both steepest energy index and flattest energy index sources, each of which are dominated by fewer individual regions. This is contradicted by the present observations, unless the Soft X-ray flat quasars become still flatter (and more variable) above 2 keV. High energy X-ray spectroscopy and variability studies are again needed to obtain a definitive answer. A RossiXTE monitoring campaign of 4 PG quasars, with a sampling similar to that used in the HRI campaign, is in progress and could allow us to clarify this point.

7. Summary

We have studied the variability of 6 low redshift, radio quiet ‘PG’ quasars on timescales from a few thousand seconds to years using the ROSAT HRI and archive ROSAT PSPC observations. The quasars were chosen to lie at the two extreme ends of the ROSAT PSPC spectral index distribution and hence of the $H\beta$ FWHM distribution. The observation strategy of the ROSAT HRI campaign has been carefully designed to provide even sampling on these three basic timescales and to provide a uniform sampling among the quasars

We have found clear evidence that the X-ray steep, narrow $H\beta$, quasars show larger amplitude variations than the X-ray flat broad $H\beta$ quasars on timescales from 2 days to 20 days. On longer timescales we do not find significant differences between steep and flat quasars, although the statistics are poorer. We suggest that the above correlation between variability properties and spectral steepness can be explained in a scenario in which the X-ray steep, narrow optical line objects are in a higher L/L_{Edd} state with respect to the X-ray flat, broad optical line objects.

Variability on short timescale (a few hundred seconds) is also evident in the steep α_X

quasars. The HRI sensitivity allows to study the variability of the brightest of these objects down to a few hundred seconds. To investigate shorter timescale variability we will have to await missions with high throughput like AXAF and XMM.

The magnitude of the variability of steep α_x quasar does not increase on timescales longer than ≈ 10 days. In particular for PG1440+356 the power spectrum roughly follows a $1/f$ law between 10^{-3} and 10^{-6} Hz, and below this frequency flattens significantly indicating a break in the power spectrum. The frequency of the break is however ill defined, because of the insufficient sampling on timescales between 1 week and several months.

The fact that flat α_x quasars have comparable variability to steep α_x quasars at $f \sim 10^{-7}$ Hz, but significantly smaller variability on $f > 10^{-5}$ Hz suggests that the variability power spectrum of flat α_x quasars may be similar in shape to that of steep α_x quasars, but with a break point scaled to lower frequencies. The other option, that the power spectrum in flat α_x quasars is just scaled down in amplitude for all f , is less favoured by our results.

A systematic study of a significantly larger sample of quasars is called for. Such a study would allow one to test the strength and significance of the $\sigma - \alpha_x$ correlation, to establish if the differences in variability power spectra is due to a scaling of the break frequency, or of the overall variability amplitude, and to eventually understand if the $\sigma - \alpha_x$ correlation is driven primarily by L/L_{Edd} or by the black hole mass. The ideal instrument for such a study would be the ROSAT HRI, which is the only X-ray telescope which allows the required large number of short exposures.

F.F. acknowledges support from grant NAG5-3039 (ROSAT). M.E. and F.N. acknowledge support from ADP grant NAG5-3066. A.L. acknowledges support by the fund for the promotion of research at the Technion. We thank Lev Titarchuk and Dan Schwartz for useful discussions and comments.

REFERENCES

- Boller T., Brandt W.N., Fink H. 1996, A&A, 305, 53
 Boller T., Brandt W.N., Fabian A.C., Fink H. 1997, MNRAS, 289, 393
 Brandt W.N., Pounds K.A., Fink H., 1995, MNRAS, 273, L47
 Brandt W.N., Mathur S., Elvis M. 1997, MNRAS 285L25
 Chakrabarti S.K., Titarchuk L. 1995, ApJ, 455, 623
 Comastri A. et al. 1998, A&A, in press

- Cui W., Heindl W.A., Rothschild R.E., Zhang S.N. Jahoda K., Focke W. 1997, *ApJL*, 474, L57
- Czerny B., Elvis M. 1987, *ApJ*, 321, 305
- David L.P., Harnden F.R., Kearns K.E., Zombeck M.V. 1997 “The ROSAT High Resolution Imager”, Technical Rep. US ROSAT Science Data Center/SAO (http://hea-www.harvard.edu/rosat/rsdc_www/hricalrep.html)
- Di Clemente A., Giallongo E., Natali G., Trevese D., Vagnetti F. 1996, *ApJ*, 463, 466
- Ebisawa K., 1991, PhD thesis, ISAS Research Note 483
- Fiore F., Elvis M., McDowell J.C., Siemiginowska A., Wilkes B.J. 1994, *ApJ*, 431, 515
- Fiore F., Elvis M., Siemiginowska A., Wilkes B.J., McDowell J.C., Mathur S., 1995, *ApJ*, 449, 74
- Fiore F., et al. 1998a, *MNRAS*, in press
- Fiore F., Mineo T., Giallongo E., 1998b, proc. of the Symposium “The Active Sky”, ed. H. Brandt, F. Fiore, P. Giommi, L. Scarsi, Rome 21-23 Oct 1997
- Fruscione A., Cagnoni I., Papadakis 1998, *ApJ*, in preparation
- Forster K., Halpern J.P. 1996, *ApJ*, 468, 565
- Kendall M., Stuart A. 1979, *The Advanced Theory of Statistics*, MacMillan, New York
- König M., Staubert R., Timmer J. 1997, proc. of the conference “Astronomical Time Series”, Tel Aviv 1-3 Jan 1997
- George I., Nandra K., Laor A., Turner T.J., Fiore F., Mushotzky R.F., Netzer H. 1997, *ApJ*, 491, 508
- Green A.R., McHardy I.M., Letho H.J. 1993, *MNRAS*, 265, 664
- Groupe D., Beuermann K., Mannheim K., Thomas H.-C. Fink H.H., de Martino D. 1995, *A&A*, 300, L21
- Laor A., Fiore F., Elvis M., Wilkes B.J., McDowell J.C. 1994, *ApJ*, 435, 611
- Laor A., Fiore F., Elvis M., Wilkes B.J., McDowell J.C. 1997, *ApJ*, 477, 93
- Lawrence A. et al. 1997, *MNRAS*, 285, 879
- Marshall H.L., Carone T.T., Shull J.M. Malkan M.A., Elvis M. 1996, *ApJ* 457 169
- Mushotzky R., Done C., Pounds K. 1993, *Ann. Rev. A&A*, 31, 717
- Nandra K., George I.M., Mushotzky R.F., Turner T.J., Yaqoob T., 1997, *ApJ*, 476, 70
- Pounds K.A., Done C., Osborne J.P., 1995, *MNRAS*, 277, L5

Siemiginowska A., Czerny B., 1989, MNRAS 239, 289

Siemiginowska A., Fiore F., Comastri A. et al. 1998, ApJ, in preparation

Schwartz D.A., Tucker W.H., 1988, ApJ, 332, 157

van der Klis, M. 1995, in “X-ray Binaries”, ed. W.H.G. Lewin, J. van Paradijs, E.P.J. van den Heuvel, Cambridge Un. press, p. 252

Zamorani G., et al. 1984, ApJ, 278, 28

Table 2: HRI Monitoring of 3 X-ray Steep Quasars

Source	Observation Date	Exposure ^a	HRI Count-rate ^b
PG 1115+407	07/Nov/95	3.14	87 ± 6
	09/Nov/95	2.39	80 ± 6
	10/Nov/95	2.23	83 ± 7
	11/Nov/95	2.29	87 ± 7
	12/Nov/95	2.91	101 ± 6
	13/Nov/95	3.53	106 ± 6
	14/Nov/95	3.62	70 ± 5
	21/Nov/95	1.71	65 ± 7
	29/Nov/95	2.06	53 ± 6
	05/May/96	2.00	139 ± 9
PG 1402+261	05/Jan/96	1.10	380 ± 20
	11/Jan/96	4.40	329 ± 9
	12/Jan/96	3.30	422 ± 12
	14/Jan/96	4.33	331 ± 9
	15/Jan/96	3.24	304 ± 10
	18/Jan/96	3.84	170 ± 7
	25/Jan/96	4.80	204 ± 7
	20-21/Jun/96	3.86	201 ± 8
PG 1440+356	03/Jan/96	3.69	1339 ± 19
	04/Jan/96	0.56	770 ± 40
	05/Jan/96	2.66	847 ± 18
	06/Jan/96	4.02	880 ± 15
	07/Jan/96	4.35	900 ± 15
	08/Jan/96	3.99	596 ± 13
	10/Jan/96	5.51	1304 ± 16
	16/Jan/96	3.51	800 ± 15
	23/Jan/96	3.50	561 ± 13
	20/Jun/96	2.72	1276 ± 22

^a in ks; ^b in ks⁻¹

Table 3: HRI Monitoring of 3 X-ray Flat Quasars

Source	Date Obs	Exposure ^a	HRI Count-rate ^b
PG 1048+342	07/Nov/95	4.13	105 ± 5
	08/Nov/95	2.08	115 ± 8
	09/Nov/95	2.06	125 ± 8
	10/Nov/95	2.14	106 ± 8
	11/Nov/95	3.30	103 ± 6
	14/Nov/95	3.40	78 ± 5
	21/Nov/95	1.86	91 ± 8
	28-29/Nov/95	3.02	103 ± 6
	04/May/96	4.31	87 ± 5
	02/Jun/96	2.54	43 ± 5
PG 1202+281	25/Nov/95	2.59	153 ± 8
	02/Dec/95	3.51	173 ± 8
	03/Dec/95	2.19	167 ± 10
	03-04/Dec/95	2.37	164 ± 9
	04-05/Dec/95	2.32	151 ± 9
	06/Dec/95	2.09	149 ± 9
	07/Dec/95	2.33	144 ± 9
	08/Dec/95	2.84	156 ± 8
	09/Dec/95	3.03	140 ± 7
	16/Dec/95	2.10	197 ± 11
	23/May/96	3.50	99 ± 6
	21/Jun/96	4.56	62 ± 4
PG 1216+069	09/Dec/95	2.46	67 ± 6
	10/Dec/95	2.33	74 ± 6
	11/Dec/95	2.65	76 ± 6
	12/Dec/95	3.16	67 ± 5
	17/Dec/95	3.80	69 ± 5
	23/Dec/95	0.88	67 ± 10
	06/Jul/96	3.79	80 ± 5

^a in ks; ^b in ks⁻¹

Table 4: RASS and PSPC pointed observation

Source	RASS	PSPC pointed
Count-rate ^a	Date Obs	Count-rate ^a
PG1115+407	108±9	65±5
PG1402+261	133±10	195±4
PG1440+356	1028±18	367±6
PG1048+342	56±6	51±3
PG1202+281	152±10	107±3
PG1216+069	96±8	99±4

^a ‘converted’ (see text) PSPC count rates in ks⁻¹

Table 5: Source root mean square variation

name	σ_{rms}^2 (2-20 days)	σ_{rms}^2 (200-2000 days)
	10 ⁻²	10 ⁻²
Steep X-ray quasars		
PG1115+407	3.2	13.8
PG1402+261	7.3	19.1
PG1440+356	8.3	15.2
Flat X-Ray quasars		
PG1048+342	1.2	13.9
PG1202+281	0.7	9.7
PG1216+069	0.0	1.8